Liquid Crystals
Publication details, including instructions for authors and subscription information:
http://www.informaworld.com/smpp/title~content=t713926090

Ferrocene-containing liquid crystals bearing a cholesteryl unit

Daniela Apreutesei[a]; Georg H. Mehl[b]; Dan Scutaru[a]
[a] Gh. Asachi Technical University of Iasi, Faculty of Chemical Engineering, Department of Organic Chemistry, 700050 Iasi, Romania [b] Department of Chemistry, University of Hull, Hull HU6 7RX, UK

To cite this Article Apreutesei, Daniela , Mehl, Georg H. and Scutaru, Dan(2007) 'Ferrocene-containing liquid crystals bearing a cholesteryl unit', Liquid Crystals, 34: 7, 819 — 831
To link to this Article: DOI: 10.1080/02678290701478715
URL: http://dx.doi.org/10.1080/02678290701478715

Liquid Crystals, Vol. 34, No. 7, July 2007, 819–831

Ferrocene-containing liquid crystals bearing a cholesteryl unit

DANIELA APREUTESEI*†, GEORG H. MEHL‡ and DAN SCUTARU†

†Gh. Asachi Technical University of Iasi, Faculty of Chemical Engineering, Department of Organic Chemistry, 71A Bd. D. Mangeron, 700050 Iasi, Romania
‡Department of Chemistry, University of Hull, Hull HU6 7RX, UK

(*Received 26 February 2007; accepted in revised form 26 April 2007*)

The synthesis and characterization of new liquid crystalline compounds containing ferrocene azo or imino aromatic and cholesteryl units is reported. The purpose of this research was to combine the properties of metals (colour, electronic density, magnetism and polarizability) with those of chiral nematics (high birefringence and presence of physical colours) and correlate relationships between chemical structures and properties in the condensed state.

1. Introduction

There is growing interest in the synthesis of metallomesogenic functionalized materials with the expectation of introducing additional properties, e.g. optical, electrical and magnetic behaviour, to soft self-assembling systems. The introduction of a ferrocene unit to a liquid crystal system may also contribute active redox properties and planar chirality of 1,3-asymmetrically substituted derivatives [1–8]. Chiral liquid crystals are studied because of the particular properties which are often associated with such materials, e.g. fast response on switching, high birefringence and presence of physical colours. However, only few examples of chiral ferrocene-containing liquid crystals have been reported. Several examples of derivatives containing both cholesteryl and ferrocenyl units have been already reported [9]. The series contains a terminal ferrocenylphenyl unit, connected to the chiral nematic one by a flexible chain, with various lengths, l_1 (figure 1).

The presence of cholesterol induces chiral mesophases in which molecules are organized in helicoidal structures, the pitch length of which is a function of temperature, external electric field and the nature and concentration of impurities in the system. The two important properties of chiral liquid crystals, mainly determined by the helical structure, are high optical activity and the presence of physical colours. The change of the chemical structure of a chiral nematic liquid crystal determines a change of the pitch length. If a chiral nematic liquid crystal also contains a photocontrollable unit, such as an azo-aromatic group, then the liquid crystal colour could be controlled by UV light stimulation. When an azo group is present, reversible photochemical changes of the cholesteric pitch by trans–cis isomerization can occur [10].

Taking into account the advantages brought by the presence of chirality, ferrocene and azo units, these structures could be good precursors in obtaining materials capable of responding to magnetic and electric fields or to UV light exposure. For this purpose, different kinds of cholesteryl-containing ferrocene derivatives were synthesized and investigated, the ferrocenyl and cholesteryl units being connected by a rigid aromatic group or via a flexible spacer.

This study is an extension of our previous research in which a ferrocene group has a flexible spacer connected to the mesogenic unit (compounds of type I, figure 2) [11]. The synthesized compounds contain a ferrocenyl unit, rigidly connected to the mesogenic part, and a cholesteryl moiety, flexibly attached by a long alkyl chain (compounds of type II, figure 2).

2. Results and discussion

2.1. *Synthesis*

The synthetic strategy for obtaining ferrocenomesogens of type II is based on the synthesis of different structural units followed by a convergent assembly of the target molecules in the final step. Ferrocene derivatives were thus obtained by either esterification of the acidic ferrocene derivatives with phenol-type units, in the presence of DCC/DMAP, or by condensation reactions of ferrocene-containing amines with cholesteryl-containing aldehydes (schemes 1 and 2).

---

*Corresponding author. Email: dapreut@ch.tuiasi.ro

Liquid Crystals
ISSN 0267-8292 print/ISSN 1366-5855 online
http://www.tandf.co.uk/journals
DOI: 10.1080/02678290701478715

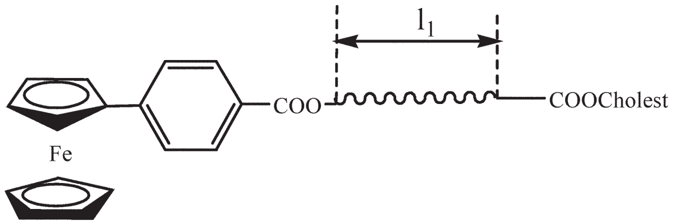

Figure 1. Ferrocene derivatives synthesized by Nakamura *et al.* [9].

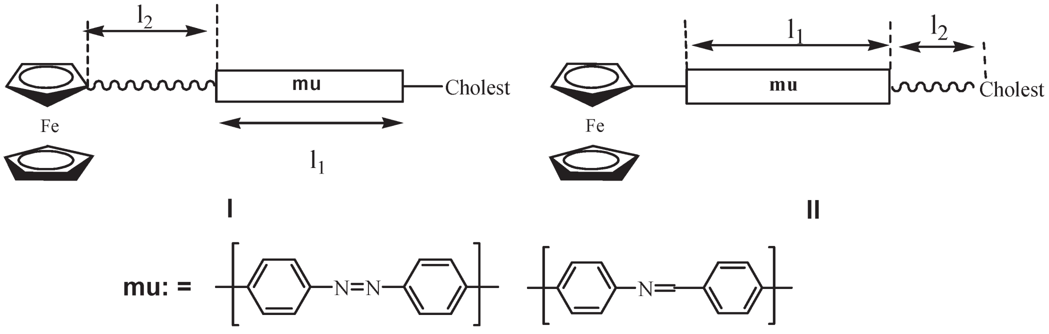

Figure 2. Ferrocene derivatives decorated with cholesteryl unit.

The ferrocene acid (**Fc$_1$**) was obtained by ferrocene arylation with the diazonium salt of 4-aminobenzoic acid with TBAI as a phase transfer catalyst (scheme 3), as reported by Zhao *et al.* [12].

Ferrocene amine (**Fc$_2$** and **Fc$_3$**) intermediates were obtained from the RNO_2 analogues, by reducing the nitro group with tin chloride or sodium sulfide (scheme 4). The nitro derivatives were synthesized either by ferrocene arylation, in conditions of phase transfer catalysis, or by esterification of the ferrocene acid or phenol with phenol or acids containing nitro groups in the presence of DCC/DMAP.

The intermediate mesogenic unit containing a phenol function, decorated with cholesterol, was obtained by reacting the silver salt of the 4-(4-hidroxyphenylazo)-benzoic acid (**5**) with the derivative **7** in dry diethyl ether (scheme 5).

The synthesis of the aldehyde type mesogenic unit **I$_2$** is presented in scheme 6.

2.2. *Mesomorphic properties and textures*

2.2.1 Properties of the intermediates. Intermediates containing a cholesteryl unit connected with a flexible spacer to the mesogenic part form a chiral nematic liquid crystal phase. Studies using polarizing optical microscopy (POM) confirmed the specific ''oily streak'' and planar textures of the chiral nematic mesophase.

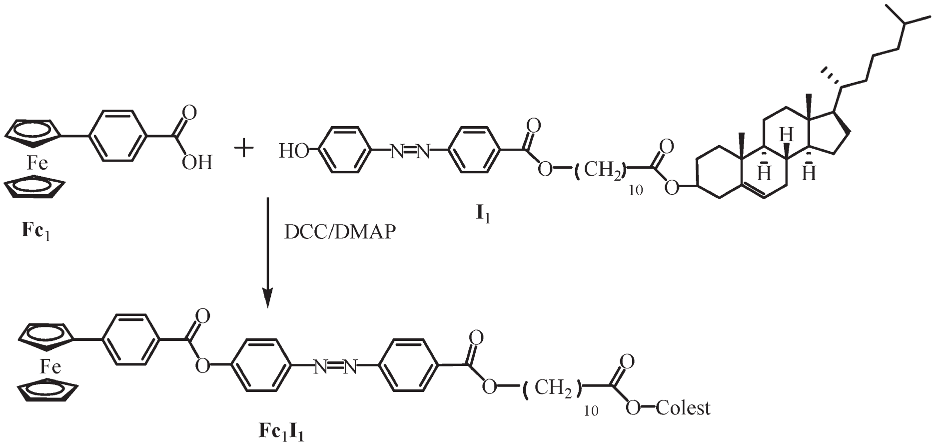

Scheme 1. Synthesis of ester linked derivative.

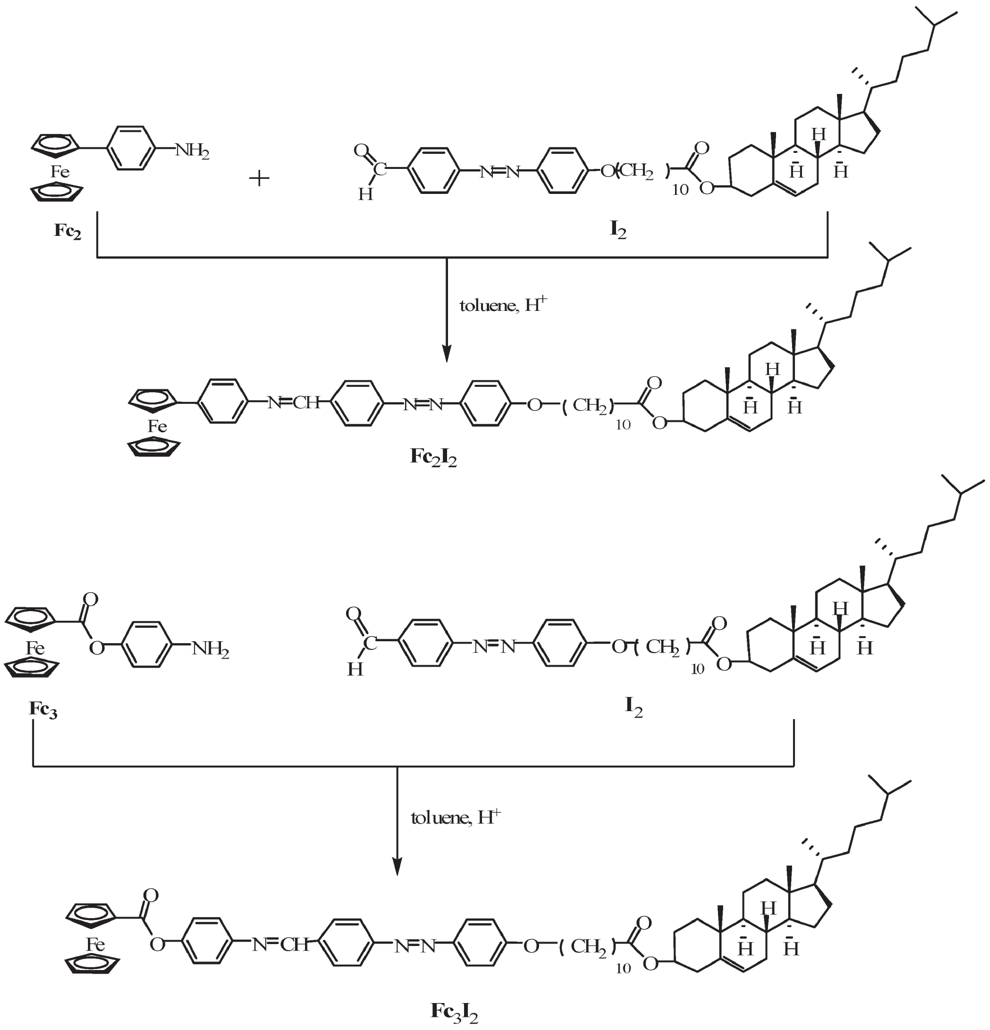

Scheme 2. Synthesis of imine-linked ferrocene derivatives.

The existence of chirality was confirmed by microscopic study of the textures and the observance of a selective turning of the apparent colour when the polarizer was turned to the left and to the right by similar values (left and right turned polarizers result in different colours). Compound $\mathbf{I_2}$, with the cholesterol group connected to the azo mesogenic unit by a chain containing ten methylene groups, forms a liquid crystalline phase in the temperature domain 101–153°C.

The analysis of the $\mathbf{I_2}$ derivative by POM shows the presence of the typical oily streak texture of the chiral nematic mesophase, but also the occurrence of a texture

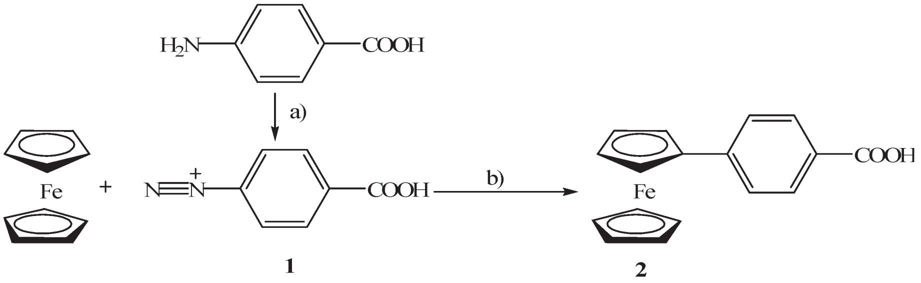

a) $NaNO_2$, HCl, 0–5ºC; b) TBAI, diethyl ether

Scheme 3. Synthesis of ferrocene acid $\mathbf{Fc_1}$.

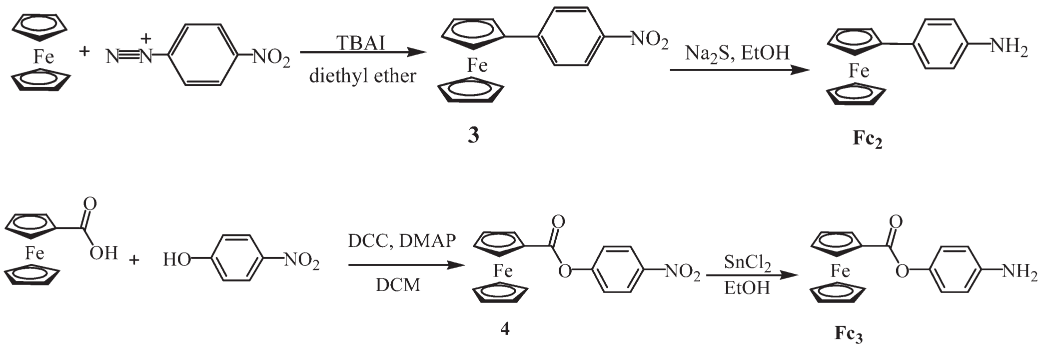

Scheme 4. Synthesis of ferrocene amines

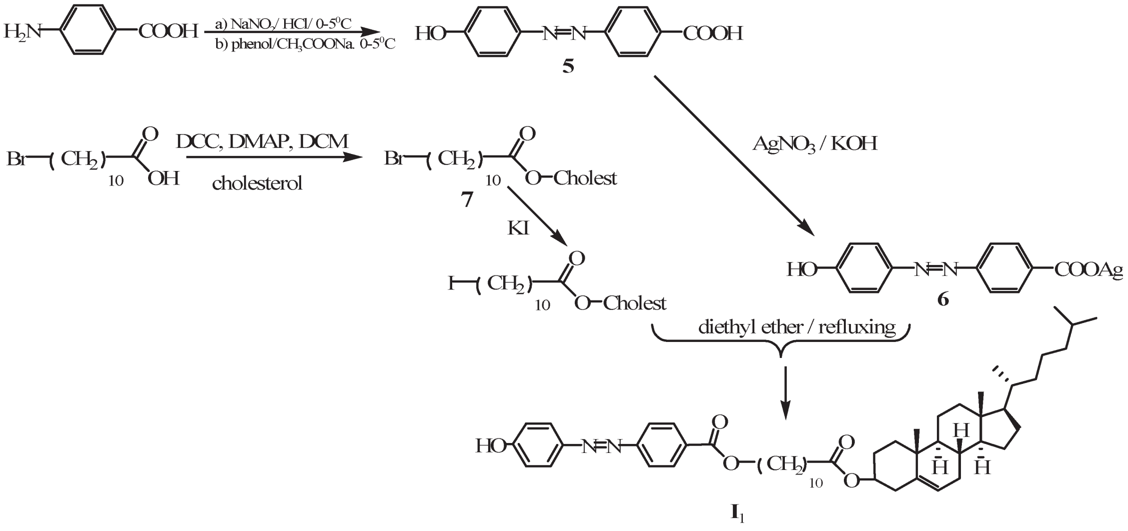

Scheme 5. Synthesis of phenol-type cholesteryl intermediate.

with pseudo focal conic defects very close to the clearing point. The textures for $\mathbf{I_2}$ are shown in figure 3.

Differential scanning calorimetry (DSC) curves of compound $\mathbf{I_2}$, shown in figure 4, confirm the existence of the mesophase and are in agreement with the observations made by optical microscopy. The phase transitions and the accompanying transition enthalpies are presented in table 1.

2.2.2. Properties of the final compounds. The connection of a cholesteryl unit to the mesogenic core by a flexible spacer (type II ferrocene derivatives) induces the appearance of smectic mesophases. This is attributed to be a consequence of the intense lateral interactions between the rigid parts. The TGB mesophase observed in ferrocene derivatives of type I was completely suppressed [11]. A decrease of the

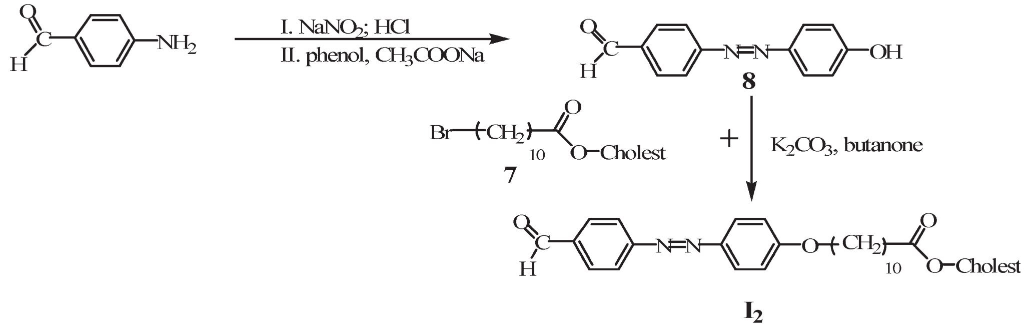

Scheme 6. Synthesis of aldehyde-type cholesteryl intermediate.

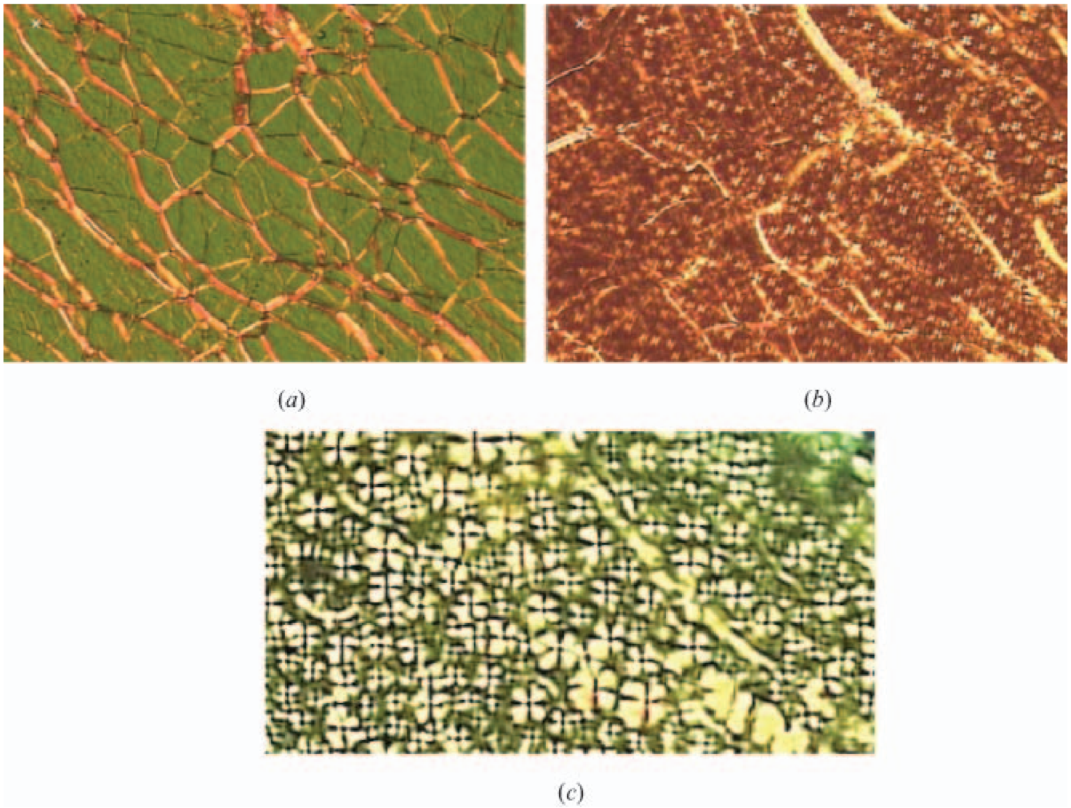

Figure 3. Textures of sample $\mathbf{I_2}$, third heating and annealing at (a) T=135.0°C, (b) T=151.2°C and (c) T=151.3°C.

clearing points, below the decomposition temperatures, if compared with type I derivatives, was also detected.

POM analysis of the ester derivative containing three aromatic rings, $\mathbf{Fc_1I_1}$, revealed an interesting liquid crystalline behaviour. The compound melts on heating at 153°C into the chiral nematic mesophase. A typical "oily streak" texture is formed and this texture remains stable until the mesophase clears at 179°C into an isotropic liquid. A typical defect texture is shown in figure 5a. On cooling from the isotropic to the chiral nematic phase, an oily streak texture is formed when the sample is sheared uniaxially (e.g. by moving the cover slip with a spatula). Figure 5b shows the formation of cholesteric texture on cooling. It is noted, however, that if the sample is annealed for more than 30 min in the chiral nematic phase close to the transition temperature, a pseudo focal conic texture appears (figure 5c) which can easily identified as a SmA phase. At 154°C, a transition to a not very specific smectic-like texture was observed (figure 5).

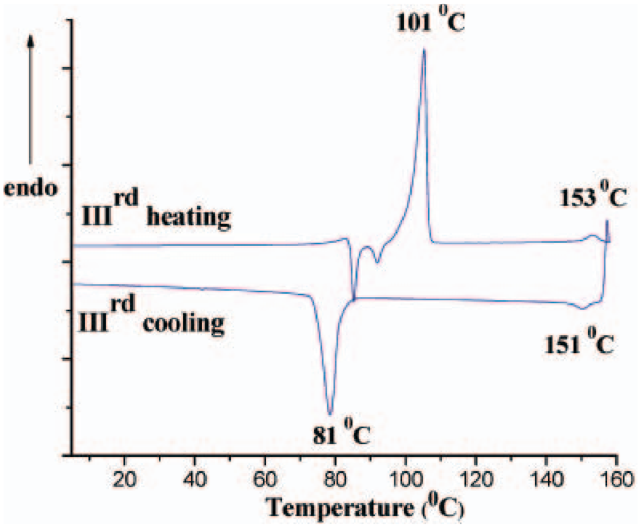

Figure 4. DSC curves of sample $\mathbf{I_2}$ in the third heating–cooling cycle, 10°C min^{-1}.

Table 1. Phase transitions of compound $\mathbf{I_2}$.

Thermal cycle	Phase transition	Temperature/°C	Enthalpy, ΔH/kJ mol^{-1}
Third heating	Cr_1–Cr_2	87.50	20.09
	Cr_2–Ch	101.34	44.05
	Ch–I	152.89	1.51
Third cooling	I–Ch	150.25	−1.49
	Ch–Cr	81.27	−36.55

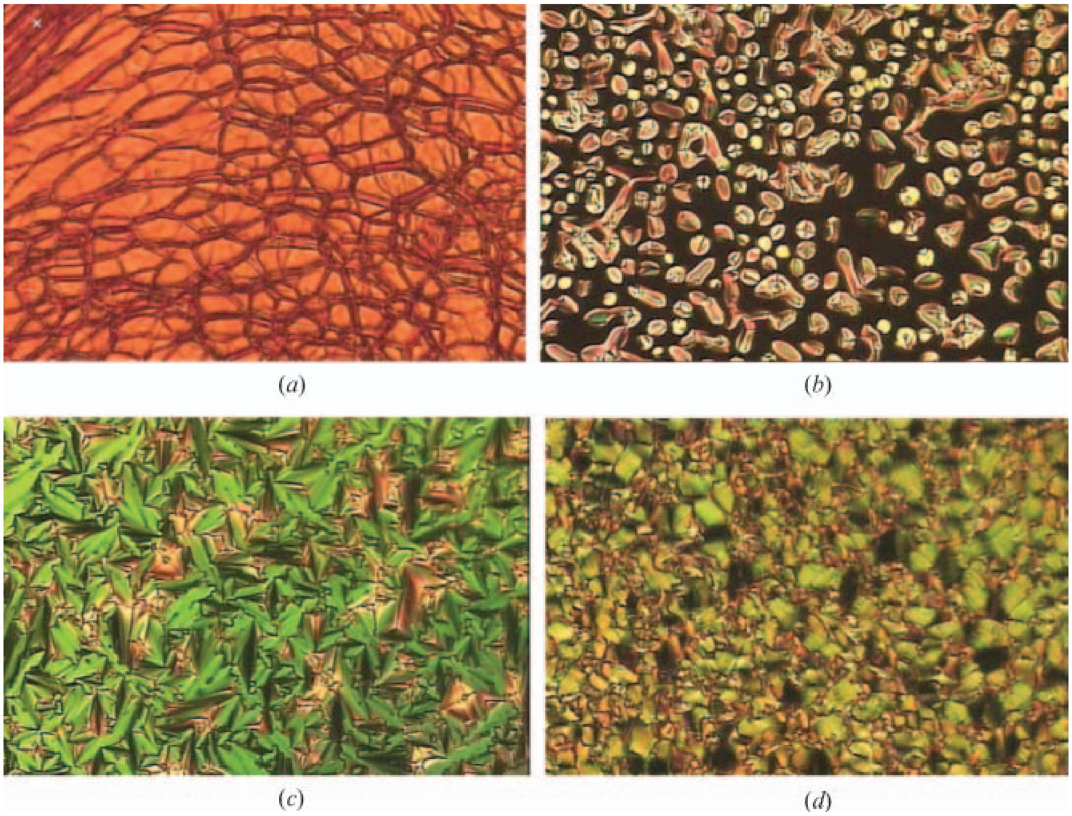

Figure 5. Textures of sample $\mathbf{Fc_1I_1}$ (second heating–cooling cycle, with 10°C min^{-1} and annealing): (a) T=164.9°C (heating); (b) T=178.6°C (cooling); c) T=174°C (cooling); (d) T=146°C.

The DSC curves for compound $\mathbf{Fc_1I_1}$ (figure 6) show the characteristic peaks of the crystal to liquid crystal transitions, characterized by high values for the transition enthalpy and those for the liquid crystal to liquid phase transition, with smaller values. The transition to the unidentified higher ordered LC phase is associated with a very small enthalpy change (ΔH=0.5 kJ mol^{-1}). This is indicative of only a small symmetry change between the two mesomorphic registers [13]. It is noted that this phase is not thermodynamically stable and could only be observed on cooling.

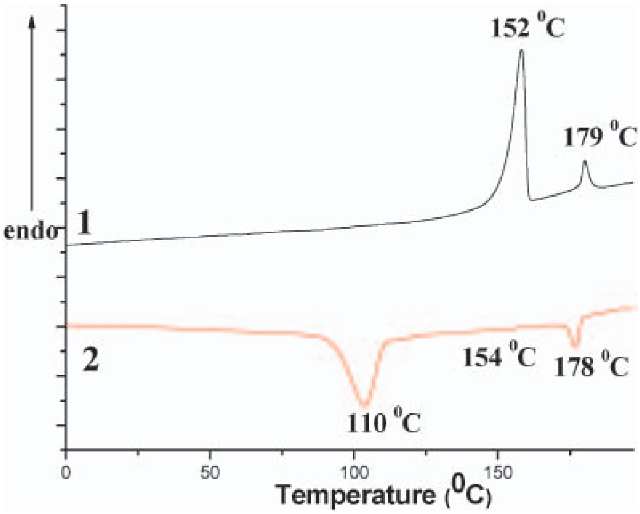

Figure 6. DSC curves of compound $\mathbf{Fc_1I_1}$ (third heating–cooling cycle, at a rate of 10°C min^{-1}).

A POM study of compound $\mathbf{Fc_2I_2}$ confirms the mesophase behaviour. On heating, $\mathbf{Fc_2I_2}$ melts at 177°C into the chiral nematic mesophase and clears at 214°C to an isotropic liquid. On cooling, the transition to the chiral nematic mesophase was observed at 213°C, followed by a transition to a monotropic smectic A phase (only stable on cooling, stability range 176°C to 135°C), characterized by a typical fan shaped texture. Typical textures for $\mathbf{Fc_2I_2}$ are shown in figure 7.

DSC studies of compound $\mathbf{Fc_2I_2}$ confirm the phase transitions observed by POM. A typical heating and cooling cycle is shown in figure 8. On cooling the chiral nematic–smectic transition could be detected, a transition enthalpy of 0.33 kJ mol^{-1} is associated with this monotropic transition.

Material $\mathbf{Fc_3I_2}$ exhibits only a chiral nematic mesophase, confirmed by POM analysis. The compound melts at 179°C (transition from crystal to chiral nematic

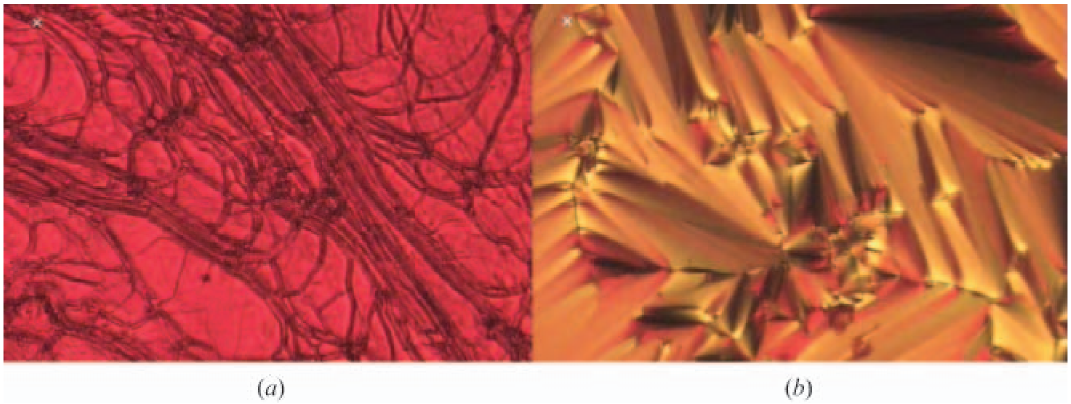

Figure 7. Textures of sample **Fc$_2$I$_2$** (second heating–cooling cycle, annealing) at (a) T=202°C and (b) T=167°C.

mesophase) and clears at 220°C (transition from chiral nematic to isotropic liquid). On cooling the isotropic to cholesteric transition could be supercooled to 218°C and the material crystallizes at 151°C. A typical oily streak texture, observed using POM, which is specific to the chiral nematic mesophase is shown in figure 9.

DSC analysis of ferrocene derivative **Fc$_3$I$_2$** confirmed the mesomorphic behaviour and the presence of two peaks corresponding to the crystal–liquid crystal and liquid crystal–liquid transitions (figure 10).

The phase structures of the two compounds (**Fc$_1$I$_1$** and **Fc$_2$I$_2$**) exhibiting smectic mesophases in the POM analysis were investigated further by X-ray diffraction (XRD). The studies proved to be challenging, as the materials tended to show partial crystallization (occurrence of "sharp" reflections in the wide-angle region), when kept over extended periods of time in the

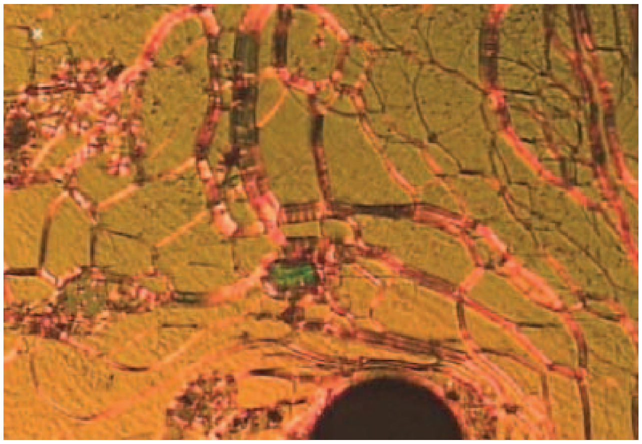

Figure 9. Texture of sample **Fc$_2$I$_2$** at T=214°C (second heating).

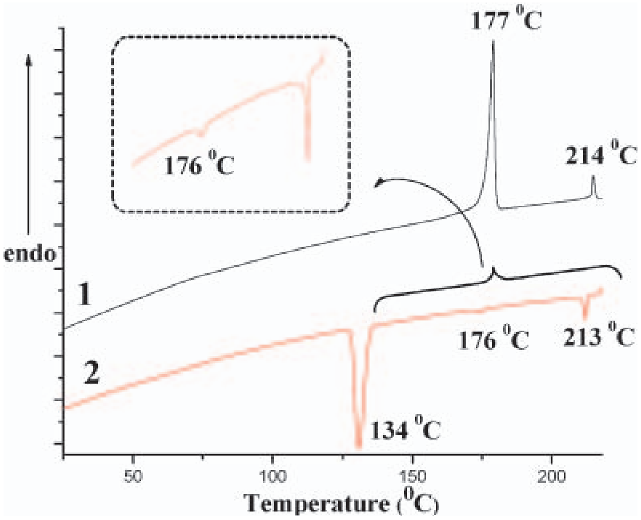

Figure 8. DSC curves of compound **Fc$_2$I$_2$** (third heating–cooling cycle, rate 10°C min^{-1}); the insert shows and expansion of the cooling trace.

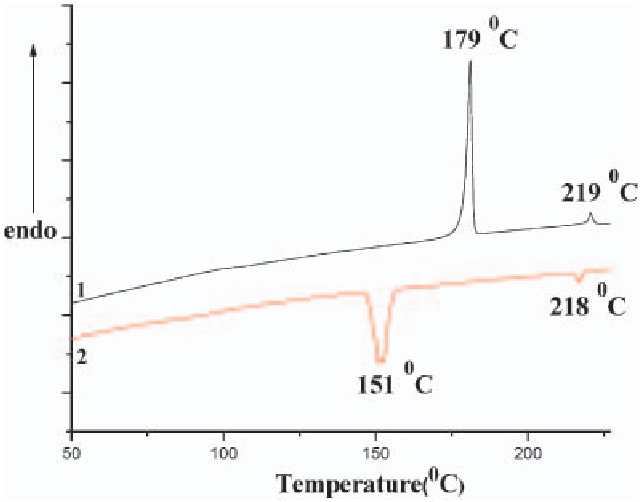

Figure 10. DSC curves of compound **Fc$_3$I$_2$** (third heating–cooling cycle, rate 10°C min^{-1}).

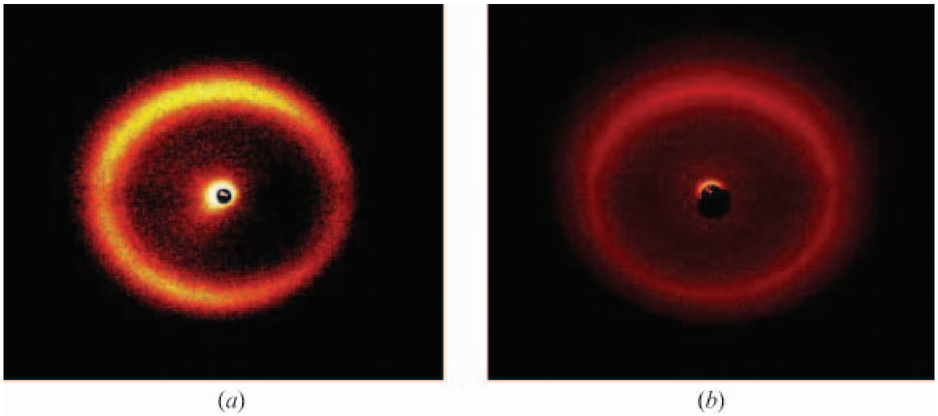

(*a*) (*b*)

Figure 11. XRD patterns for compound $\mathbf{Fc_1I_1}$ (a) and $\mathbf{Fc_2I_2}$ (b), both supercooled to 25°C.

thermodynamically unstable smectic phases. Thus, the materials were cooled in Lindemann capillaries from the chiral nematic phase to the smectic phase and than quenched to 25°C where a smectic glass is formed. Based on the POM and DSC investigations it is assumed that no further LC phases are formed during this process, or in other words that the symmetry of the phase structure of the supercooled samples is that of the monotropic smectic phases. The typical diffractograms collected for $\mathbf{Fc_1I_1}$ and $\mathbf{Fc_2I_2}$ are shown in figure 11.

The radially integrated XRD patterns of compounds $\mathbf{Fc_1I_1}$ and $\mathbf{Fc_2I_2}$ are presented in figure 12.

The diffractograms are characterized by broad, diffuse reflection in the wide-angle regions and a sharper small-angle reflection with somewhat higher intensity. No significant preferential orientation of the LC phase in the capillary mediated either through flow filling of the capillaries or by an external magnetic field could be detected. Essentially the diffractograms are powder samples of low-ordered anisotropic fluids. For $\mathbf{Fc_1I_1}$ a typical diffuse reflection centred at (q=1.2) 5.1 Å, corresponding to the lateral distances of the organic anisotropic fluid is found. This value is slightly larger than that observed typically for most calamitic systems, where often values between 4.4 Å and 5 Å are reported. However, when the terminal bulky ferrocene group and the laterally substituted aromatic group in the linear aromatic mesogen are considered (these groups are incidentally the most electron rich and thus contribute strongly to the scattering), which extend the rotational envelope of the molecule, the value of 5.1 Å, for the average lateral distance of the molecules is less surprising. At small angles a reflection at q=0.08, indicative of a register with a periodicity of d=66.3 Å, is detected, which is associated with the smectic layering. It is notable that the observed intensity of the small-angle reflection is not much larger than that for the diffuse wide-angle scattering, indicative of very weak

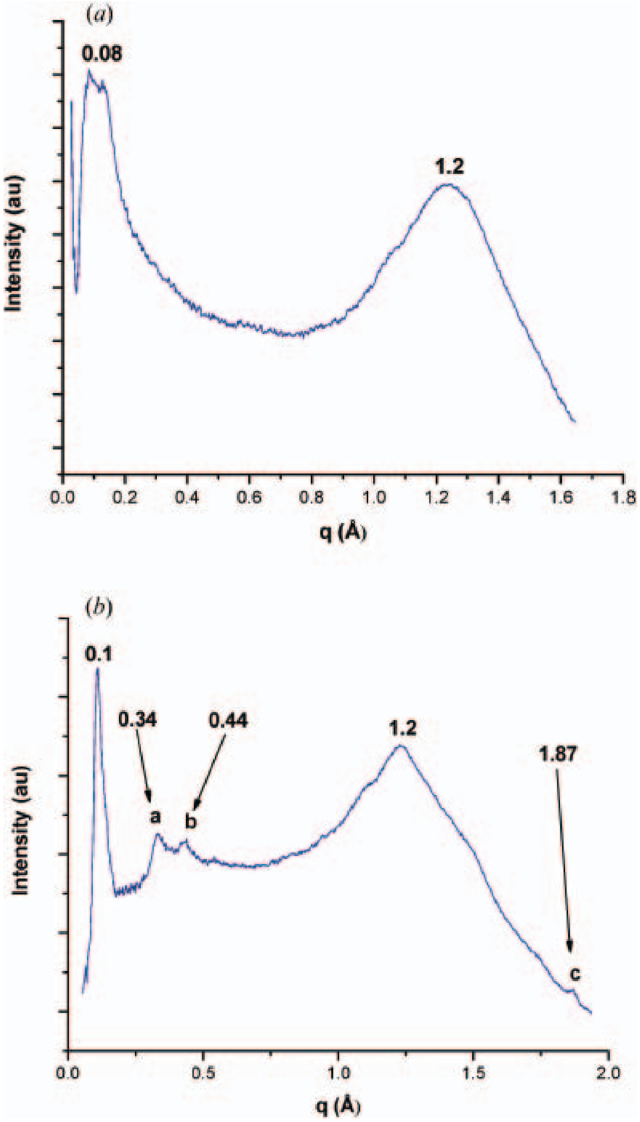

Figure 12. Radially integrated XRD patterns of compounds $\mathbf{Fc_1I_1}$ (a) and $\mathbf{Fc_2I_2}$ (b), supercooled to 25°C.

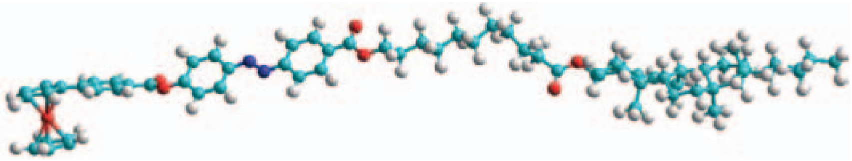

Figure 13. Geometry of compound **Fc$_1$I$_1$**, determined from HyperChem molecular modelling at the molecule minimum of energy.

positional ordering, or in other words the layering is very weak. As the *d* value is greater than molecular length *l*, estimated to be 51 Å in an all-trans conformation (a model of the molecule is shown in figure 13), some type of interdigitated layer formation has to occur. The value of *d*/*l* ~1.3 is too large to be accommodated by a disordered monolayer; however, smaller *d*/*l* values of 1.5–1.6 are typically associated with interdigitated low molar mass systems [14].

Figure 14 shows a schematic suggestion for the layering and thus a model between the typical interdigitated layer and a single-layer SmA phase is required. A possible solution is shown in figure 14. The aromatic groups are placed at the interfaces of the layers, due to microphase separation, steric requirements and attractive anisotropic polarizabilities of the aromatic groups. The aliphatic chains and the mainly hydrocarbon groups containing cholesteryl mesogen are interdigitated in the centre of the layers. It should, however, be noted that this simple model is likely to have only a slightly higher probability of being formed than other similar arrangements, thus explaining the weakness of the layering and additionally the lack of thermodynamic stability of the SmA phase.

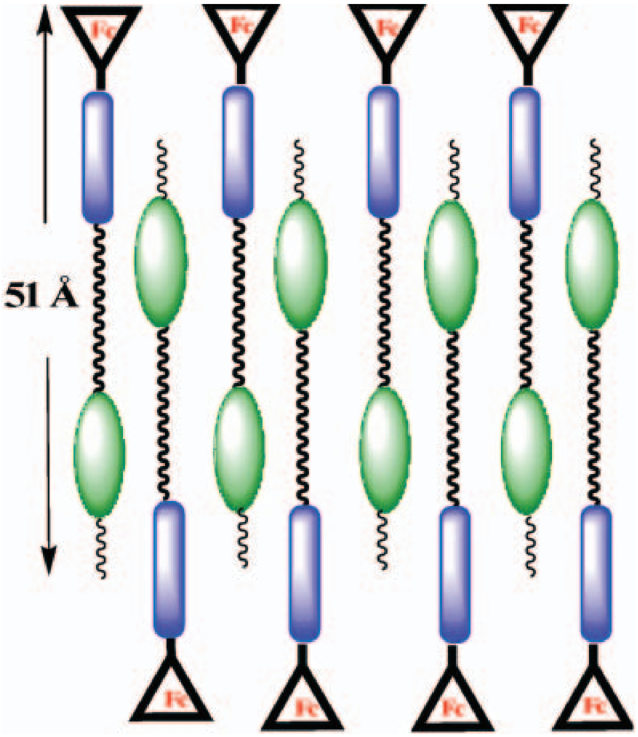

Figure 14. Probable supramolecular ordering of compound **Fc$_1$I$_1$** in the smectic mesophase.

The diffraction pattern for **Fc$_2$I$_2$** (figure 11b) shows broadly speaking similar features as those discussed above for **Fc$_1$I$_1$**. A strong diffuse wide-angle scattering at (q=1.2) 5.1 A, and a small-angle signal at (q=0.1) 63.1 Å were detected. The radial integration depicted in figure 12b shows additionally a number of small peaks (labelled a, b, c). The occurrence of a wide-angle peak (c at q=1.87, 3.6 Å) in particular suggests a well-defined intermolecular register at short ranges, or in other words, the sample shows the onset of partial crystallization and the peaks a, b, c record this process. This observation makes any structural discussion more tentative; however, some qualitative considerations are still possible. The comparison of the intensities between small-angle and wide-angle signals suggests a weak layering. A comparison of the *d* spacing of 63.1 Å with estimated length of the molecule of 51 Å yields a *d*/*l* ratio of ~1.2, which is in line with the values observed typically for low-ordered monolayer (SmA) phases. Additionally, the Schiff base linking group is more rigid than the ester group in **Fc$_1$I$_1$**, thus leading to a slightly different packing behaviour. A comparison of the two systems suggests that the change from an ester linking group to a Schiff base shifts the assembly register in the SmA phase going from a SmA$_d$ phase towards a monolayer SmA phase organization.

2.3. *Influence of molecular structure on mesomorphic mesophase*

The study of the influence of the molecular structure on mesomorphic properties of type II ferrocene derivatives has the objective of elucidating the relationship between molecular structure and mesomorphic behaviour in these systems [15].

As a general observation, the separation of cholesteryl and aromatic mesogenic units by a spacer of ten methylene units favours the formation of layered phases at low temperatures. This is attributed to enhanced flexibility of such systems, essentially converting them to non-symmetrical dimmers. Noticeable is disappearance

Table 2. Mesomorphic properties of the type-II ferrocene derivatives.

Sample	Phase transition	Temperature/°C	Enthalpy, ΔH/ kJ mol^{-1}
Fc_1I_1	Cr–Ch	152.1	31.52
	Ch–I	178.9	3.69
	I–Ch	177.9	−2.94
	Ch–Sm	153.9	−0.54
	Sm–Cr	110.0	−24.77
Fc_2I_2	Cr–Ch	176.6	37.79
	Ch–I	214.2	1.92
	I–Ch	212.7	−2.11
	Ch–S_A*	176.0	−0.33
	S_A*–Cr	134.3	−38.5
Fc_3I_2	Cr–Ch	179.0	33.66
	Ch–I	219.6	1.26
	I–Ch	218.1	−1.38
	Ch–Cr	151.2	−32.07

of the TGB phase for such compounds, which occurs in structurally related systems [11]. The properties of the ferrocene derivatives of this report are summarized in table 2.

2.4. *Influence of connecting groups and nature of aromatic rings*

Although the structural changes are minor, the overall length of the molecules varies only by 2–3 Å and this is mainly due a variation in rigidity in the aromatic part of the molecule, a different mesophase behaviour of the compounds **Fc_1I_1**, **Fc_2I_2** and **Fc_3I_2** was detected. The change in one ester linking group in **Fc_1I_1** to an imine link in **Fc_1I_1** results not only in very different isotropization temperatures, 178.9°C for **Fc_1I_1** to 214.2°C for **Fc_2I_2** (a difference of 35.9°C), but also a difference in the onset of the SmA phase 153.9°C for **Fc_1I_1** and 176.0°C for **Fc_2I_2** (a difference of 22.1°C). Furthermore, the organization of the molecules in the layered phase is subtly different, with **Fc_2I_2** tending more towards single-molecule layer formation, whereas for **Fc_1I_1** some tendency towards a strongly interdigitated bilayer can be detected. In conclusion, small changes in the flexibility and the polarity of the linking groups modifies the stability of the condensed phase and controls the occurrence of higher ordered layered phases at lower temperatures and their mode of self-organization.

3. Conclusions

New liquid crystalline compounds containing ferrocene, azo, imino and cholesteryl units were prepared. All synthesized ferrocene derivatives exhibit liquid crystalline properties, with a chiral nematic (chiral nematic) phase as the highest stable mesophases. Controlled changes of the linking groups at relevant positions in the molecules lead to significantly different transition temperatures, the formation of smectic phase behaviour (SmA) and a modulation in the assembly behaviour in the smectic phase. This phase behaviour was explored using POM, DSC and by XRD studies and rationalized in terms of spatial requirements and the flexibility of the crucial linking group.

4. Experimental

4.1. *Materials*

All materials were used as purchased unless otherwise mentioned. All reactions involving DCC and DMAP were performed under a dry atmosphere of nitrogen. Silica gel 60 (Merck) or Al_2O_3 (active, neutral, Merck) were used for column chromatography. TLC was performed on silica gel or Al_2O_3 plates (Merck, Silicagel F254, aluminium oxide F254). The synthesis and thermal properties of the corresponding ferrocene amines has been reported previously [16]. The synthesis of 4-ferrocenylbenzoic acid was performed by using a literature method [17].

4.2. *Instrumentation*

Nuclear magnetic resonance (NMR) spectra were recorded on a Jeol JNM-ECP 400 MHz FT-NMR spectrometer. Chemical shifts are reported in ppm relative to TMS. Thermal properties were investigated using a Mettler Toledo differential scanning calorimeter (DSC 822e) in nitrogen against an indium standard. Transition temperatures were determined as the onset of the maximum in the endotherm or exotherm. The mesophases were studied on an Olympus BH-2 polarizing optical microscope, equipped with a Mettler FP82 HT hot stage and a Mettler FP90 central processor. Pictures of the mesophases were taken using a JVC digital video camera connected to a PC. Software Studio Capture, supplied by Studio86Designs, was used for image capturing. XRD studies were performed on MAR345 diffractometer, equipped with 2D images detector, CuKα radiation source, graphite monochromator, λ=1.54 Å.

4.3. *Synthesis*

4.3.1. 4-(4-hydroxyphenylazo)benzoic acid (5). To a solution of 4-aminophenol (1 eq), hydrochloric acid (3 eq) was added. The mixture was cooled on an ice bath to 0°C and a solution containing $NaNO_2$ (1 eq) in H_2O (20%) was added, under stirring, keeping the temperature below 5°C. The diazonium salt was maintained at 5°C for an additional 30 min. The diazonium salt was then added dropwise to a solution containing phenol (1.03 eq) and $CH_3COONa.3H_2O$ (10 eq), in water (5 ml), at 5°C. The orange precipitate was filtered off and washed several times with water. Yield: 90%; m/z 242 [M]+.

4.3.2. Silver 4-(4-hydroxyphenylazo)benzoate (6). 4-(4-hydroxyphenylazo)benzoic acid (0.22 g, 0.9 mmol) was added to a solution of KOH (0.05 g in 3 ml H_2O). The solution was slowly heated until salt formation was observed (the solution became clear). After cooling, a solution of $AgNO_3$ (8%, 0.15 g $AgNO_3$ in 4.12 ml distilled water) was added slowly, under stirring. The brown silver salt was filtered off, washed several times with distilled water and used without further purifications. ^1H NMR, δ (DMSO): 8.11 (d, 2H, Ar), 7.84 (d, 4H, Ar), 6.97 (d, 2H, Ar), 5.60 (s, 1H, –OH). ^{13}C NMR, δ (DMSO): 160.98, 153.49, 145.24, 135.93, 130.01, 124.57, 124.48, 121.20, 115.74. m/z: 398 [M-1]+.

4.3.3. Cholesteryl 10-bromoundecanoate (7). To a solution containing 11-bromoundecanoic acid (2 g, 7.19 mmol), cholesterol (2.78 g, 7.19 mmol) and a catalytic amount of DMAP in anhydrous DCM, under stirring, a solution of DCC (1.63 g, 7.91 mmol) dissolved in dried CH_2Cl_2 was added. After 18 h of stirring, the dicyclohexylurea was filtered off and the solution was concentrated. The solid residue was purified by column chromatography (CC) on Al_2O_3 (DCM:hexane=1:1) and crystallized from ethanol to give a white powder. Yield: 4.41 g (95%); m.p. 95°C. IR (KBr, cm^{-1}): 2931, 2852 (C–H), 1734 (>C=O, esteric), 1465, 1379, 1321, 1247, 1168, 1026, 1001, 956, 920, 940, 800, 725, 646, 594, 565. ^1H NMR, δ ($CDCl_3$): 5.36 (d, 1H, –C=CH–), 4.60 (m, 1H, COO–CH–), 3.39 (t, 2H, Br–CH_2–), 2.29 (t, 2H, –CH_2–), 2.25 (t, 2H, –CH_2–), 2.01–0.84 (m, 56H, aliphatic protons), 0.66 (s, 3H, –CH_3). ^{13}C NMR, δ ($CDCl_3$): 173.2, 139.64, 122.54, 73.61, 56.63, 56.07, 49.96, 42.25, 39.67, 39.47, 38.11, 36.95, 36.53, 36.13, 35.75, 34.63, 33.95, 32.77, 31.85, 31.80, 29.31, 29.28, 29.16, 29.03, 28.69, 28.19, 28.11, 27.96, 27.76, 24.98, 24.23, 23.78, 22.79, 22.53, 20.98, 19.28, 18.66, 11.80. m/z: 632 [M-1]+.

4.3.4. Cholesteryl 10-[4-(4-carboxyphenylazo)phenol]-undecanoate (I_1). For synthesis of the iodo derivative, **7** (0.11 g, 0.17 mmol), NaI (0.03 g, 0.26 mmol) and 20 ml acetone were refluxed for 5 h. After cooling, the solvent was removed and the resulting compound used for the next step without further purification. For synthesis of intermediate I_1, a mixture of **6** (0.24 g, 0.7 mmol) and the iodo derivative (0.45 g, 0.69 mmol) in diethyl ether was refluxed for 48 h under a nitrogen atmosphere. The solution was concentrated under vacuum and the crude compound was purified by CC, using a DCM:hexane 10:1 mixture as eluent to give an orange powder. Yield 0.11 g (19.55%). m/z: 795 [M]+.

4.3.5. 4-(4-Hydroxyphenyazo)benzaldehyde (8). To a solution of 4-aminobenzaldehyde (2.3 g, 19 mmol), hydrochloric acid (5.9 ml) was added. The mixture was cooled on an ice bath to 0°C and a solution containing $NaNO_2$ (1.31 g, 26.6 mmol) in 5 ml H_2O (20%) was added, under stirring, keeping the temperature below 5°C. The diazonium salt was maintained at 5°C for an additional 30 min before being added dropwise to a solution containing phenol (1.84 g, 19.55 mmol), $CH_3COONa.3H_2O$ (4.39 g, 0.195 mol) and 18 ml water at 5°C. After 3 h, the orange precipitate was filtered off and washed several times with water. Yield: 3.61g (84%). ^1H NMR, δ ($CDCl_3$): 10.09 (s, 1H, –CH=O), 8.00 (dd, 4H, Ar), 7.92 (d, 2H, Ar), 6.97 (d, 2H, Ar), 1.53 (s, 1H, –OH). ^{13}C NMR, δ (CDCl3): 191.93, 130.84, 125.70, 123.82, 123.17, 116.08l. m/z: 226 [M+].

4.3.6. Cholesteryl 11-[4-(4-formylphenylazo)phenoxy]-undecanoate (I_2). A mixture of **8** (1 eq), **7** (1.5 eq), K_2CO_3 (1.5 eq), KI (0.5 eq) and butanone was refluxed overnight. The mixture was allowed to cool to room temperature, the solids were filtered off, washed thoroughly with warm acetone and the solvent was evaporated under reduced pressure. Purification was achieved by CC using a CH_2Cl_2:hexane 3:1 mixture as eluent. Crystallization from methanol gave an orange powder. Yield: 64%. ^1H NMR, δ ($CDCl_3$): 10.09 (s, 1H, –CH=O), 8.01 (m, 6H, Ar), 7.02 (d, 2H, Ar), 5.37 (d, 1H, –C=CH–), 4.60 (m, 1H, COO–CH–), 4.05 (t, 2H, –CH_2–), 2.29 (t, 2H, –CH_2–), 2.27 (t, 2H, –CH_2–), 2.01–0.84 (m, 56H, aliphatic), 0.66 (s, 3H, –CH_3). ^{13}C NMR, δ ($CDCl_3$): 191.69, 173.34, 162.67, 156.26, 146.96, 139.76, 137.01, 130.77, 125.49, 123.14, 122.69, 114.91, 73.76, 68.53, 56.73, 56.21, 50.07, 42.37, 39.79, 39.61, 38.26, 37.08, 36.66, 36.27, 35.89, 34.77, 31.97, 31.92, 29.81, 29.55, 29.44, 29.32, 29.25, 29.17, 28.32, 28.10, 27.91, 26.08, 25.13, 24.36, 23.94, 22.94, 22.68, 21.11, 19.41, 18.81, 11.94.

4.4. *Synthesis of ferrocene derivatives Fc_1I_3, Fc_2I_2 and Fc_3I_2*

The synthesis was carried out by esterification with DCC, DMAP in CH_2Cl_2 or by condensation of the ferrocene amines with cholesteryl aldehydes (Schiff base synthesis) in toluene in the presence of a catalytic amount of acetic acid.

4.4.1. Cholesteryl 11-{[4-(ferrocenylbenzoyloxy)-4-phenylazo]-4-benzoyloxy}undecanoate (Fc$_1$I$_1$). To a solution containing 4-ferrocenylbenzoic acid (0.07 g, 2.93 mmol), **I$_1$** (0.11 g, 0.13 mmol) and a catalytic amount of DMAP in anhydrous CH_2Cl_2, was added, under stirring, a solution of DCC (0.032 g, 0.156mmol) dissolved of dried CH_2Cl_2. After 24 h of stirring, dicyclohexylurea was filtered off and the solution was concentrated. The solid residue was purified by CC on silica gel, using a CH_2Cl_2:hexane 1:1 mixture as eluent, yielding a red-orange powder. Yield: 0.09 g (67%). IR (KBr/cm^{-1}): 2929.86, 2850.78 (C–H), 1930.74, 1726.29 (>C=O), 1647.21, 1602.84, 1523.76, 1492.9, 1465.9, 1409.96, 1382.96, 1330.88, 1271.09, 1220.94, 1174.65, 1139.93, 1105.21, 1087.85, 1064.7, 1029.99, 1006.84, 956.69, 923.9, 885.32, 862.18, 81974, 769.6, 723.3, 696.3, 628.79, 547.78, 518.85, 472.56, 437.84, 422.4. ^{1}H NMR, δ ($CDCl_3$): 8.20 (d, 2H, Ar), 8.10 (d, 2H, Ar), 8.05 (d, 2H, Ar), 7.96 (d, 2H, Ar), 7.52 (d, 2H, Ar), 7.41 (d, 2H, Ar), 5.37 (d, 1H, –C=CH–, cholesteryl), 4.90 (t, 2H, C_5H_4–), 4.59 (m, 1H, COO–CH–), 4.31 (t, 2H, C_5H_4–), 4.19 (s, 5H, C_5H_5), 2.31 (d, 2H, cholesteryl), 2.27 (t, 1H, –CH_2–), 2.01–0.85 (59H, aliphatic), 0.68 (s, 3H, –CH_3 cholesteryl). ^{13}C NMR, δ ($CDCl_3$): 173.42, 166.21, 164.85, 155.08, 153.74, 150.24, 146.6, 139.8, 132.32, 130.69, 130.47, 126.25, 125.96, 124.58, 122.76, 122.67, 122.61, 73.78, 71.43, 71.31, 68.06, 65.56, 56.76, 56.2, 50.08, 42.39, 39.8, 39.61, 38.25, 37.08, 36.68, 36.27, 35.89, 34.81, 31.99, 31.94, 29.55, 29.48, 29.34, 29.19, 28.81, 28.33, 28.12, 27.91, 26.14, 25.15, 24.38, 23.93, 22.94, 22.68, 21.11, 19.43, 18.81, 11.95.

4.4.2. Cholesteryl 11-{[4-(ferrocenylphenylimino)methyl-4-phenylazo]-4-phenoxy}-undecanoate (Fc$_2$I$_2$). Under argon, 4-ferrrocenylaniline (0.048 g, 0.17 mmol) and aldehyde **I$_2$** (0.15 g, 0.17 mmol) were dissolved in ethanol (10 ml) and a catalytic amount of acetic acid was added. The reaction mixture was stirred under reflux for 10 h. After cooling, the product was filtered off and purified by CC on silica gel using a DCM:hexane 1:3–TEA 3% mixture. Crystallization from ethanol gave orange crystals. Yield 0.1 g (57%). ^{1}H NMR, δ ($CDCl_3$): 8.59 (s, 1H, –N=CH–), 8.05 (d, 2H, Ar), 7.96 (m, 4H, Ar), 7.49 (d, 2H, Ar), 7.23 (d, 2H, Ar), 7.02 (d, 2H, Ar), 5.37 (d, 1H, –C=CH–), 4.72 (s, 2H, ferrocene), 4.61 (m, 1H, –COO–CH–), 4.38 (s, 2H, ferrocene), 4.10 (s, 5H, ferrocene), 4.05 (t, 2H, –CH_2–), 2.29 (d, 2H, cholesteryl), 2.27 (t, 2H, –CH_2–), 2.01–0.85 (m, 57H, aliphatic), 0.66 (s, 3H, –CH_3). ^{13}C NMR, δ (CDCl3): 173.43, 162.21, 158.42, 154.40, 149.51, 147.05, 139.80, 137.85, 129.67, 126.90, 125.16, 123.10, 122.71, 121.28, 114.88, 73.78, 70.00, 69.40, 68.49, 66.65, 56.76, 56.20, 50.09, 42.39, 39.80, 39.60, 38.25, 37.08, 36.68, 36.26, 35.89, 34.80, 31.99, 31.94, 29.55, 29.44, 29.32, 29.27, 29.17, 28.32, 28.11, 27.90, 26.09, 25.14, 24.37, 23.92, 22.93, 22.67, 21.11, 19.42, 18.80; 11.90.

4.4.3. Cholesteryl 11-{[4-(ferrocenoyloxyphenylimino)-methyl-4-phenylazo]-4-phenoxy}-undecanoate (Fc$_3$I$_2$). 4-Ferrrocenylcarboxyaniline (0.03 g, 0.093 mmol) and aldehyde **I$_2$** (0.08 g, 0.093 mmol) were dissolved in ethanol (10 ml) and a catalytic amount of acetic acid was added. The reaction mixture was stirred under reflux for 18 h. After cooling, the product was filtered off and purified on silica gel using a DCM:hexane 1:5–TEA 3% mixture. Crystallization from toluene gave orange crystals. Yield 0.051 g (47%). ^{1}H NMR δ ($CDCl_3$): 8.56 (s, 1H, –N=CH–), 8,05 (d, 2H, Ar), 7.96 (m, 4H, Ar), 7.24 (d, 2H, Ar), 7.01 (d, 2H, Ar), 5.38 (d, 1H, –C=CH–), 4.98 (s, 2H, ferrocene), 4.60 (m, 1H, –COO–CH–), 4.51 (s, 2H, ferrocene), 4.32 (s, 5H, ferrocene), 4.05 (t, 2H, –CH_2–), 2.30 (t, 2H. –CH_2–), 2.27 (t, 2H, –CH_2–), 2.02-0.86 (m, 56H, aliphatic protons), 0.67 (s, 3H, –CH_3).

Acknowledgment

D.S. and D.A. gratefully acknowledge financial support from the Ministry of Education of Romania (grant 33371/2004, code CNCSIS 554/40 and grant 33371/2004, code CNCSIS 143/91).

References

[1] J. Malthête, J. Billard. *Mol. Cryst. liq. Cryst*, **34**, 117 (1976).

[2] (a) Y. Galyametdinov, O. Kadkin, V.I. Gavrilov, L.M. Tinchurina. *Russ. Chem. Bull*, **44**, 350 (1995); (b) O. Kadkin, Y. Galyametdinov, A. Rakhmatullin. *Mol. Cryst. liq. Cryst.*, **332**, 109 (1999).

[3] (a) C. Loubser, C. Imrie. *J. Chem. Soc., Perkin Trans. 2*, 399 (1997); (b) C. Imrie, C. Loubser, P. Engelbrecht, C.W. McCleland. *J. Chem. Soc., Faraday Trans. 1*, 2513 (1999); (c) C. Imrie, P. Engelbrecht, C. Loubser, C.W. McCleland. *Appl. Organomet. Chem,* **1**, 15 (2001); (d) C. Imrie, P. Engelbrecht, C. Loubser, C.W. McCleland, O.V. Nyomori, R. Bogardi, D.C. Levendis, N. Tolom, J. Rooyen, N.J. Williams. *J. Organomet. Chem.*, **645**, 65 (2002); (e) C.T. Imrie, C. Loubser, P. Engelbrecht, C.W. McCleland, Y.F. Zheng. *J. Organomet. Chem.*, **665**, 48 (2003).

[4] (a) T. Seshadri, H.J. Haupt. *J. Mater. Chem*, **8**, 1345 (1998); (b) W.-C. Shen, Y.-L. Cheng, G.-H. Lee, C.K. Lai. *Tetrahedron*, **62**, 8035 (2006).

[5] H. Adams, N.A. Bailez, D.W. Bruce, S.A. Hudson, J.R. Marsden. *Liq. Cryst*, **16**, 643 (1994).

[6] (a) R. Deschenaux, J.L. Marendaz. *J. Chem. Soc., Chem Commun*, 909 (1991); (b) R. Deschenaux, M. Rama, J. Santiago. *Tetrahedron Lett.*, **34**, 3293 (1993); (c) R. Deschenaux, I. Kosztics, U. Scholten, D. Guillon, M.J. Ibn-Elhaj. *J. Mater. Chem.*, **4**, 1351 (1994); (d) R. Deschenaux, V. Izvolenski, F. Turpin, D. Guillon, B. Heinrich. *Chem. Commun.*, 439 (1996); (e) R.

Deschenaux, I. Jauslin, U. Scholten, F. Turpin, D. Guillon, B. Heinrich. *Macromolecules*, **31**, 5647 (1998); (f) H.J. Coles, S. Meyer, P. Lehmann, R. Deschenaux, I. Jauslin. *J. Mater. Chem.*, **9**, 1985 (1999); (h) F. Turpin, D. Guillon, R. Deschenaux. *Mol. Cryst. liq. Cryst.*, **362**, 171 (2001); (i) T. Chuard, R. Deschenaux. *J. Mater. Chem.*, **12**, 1944 (2002); (j) T. Chuard, R. Deschenaux. *Chimia*, **57**, 597 (2003); (k) S. Campidelli, L. Perez, J.R. Lopez, J. Barbera, F. Langa, R. Deschenaux. *Tetrahedron*, **62**, 2115 (2006).

[7] (a) J. Andersch, C. Tschierske, S. Diele, D.J. Lose. *J. Mater. Chem*, **6**, 1297 (1996); (b) J. Andersch, C. Tschierske. *Liq. Cryst.*, **21**, 51 (1996).

[8] P.H. Zhao, K.Q. Xu, H.B. Zhang, L. Fu. *J. Chin. Chem. Soc*, **60**, 168 (2002).

[9] (a) N. Nakamura, T. Hanasaki, H. Onoi. *Mol. Cryst. liq. Cryst*, **225**, 269 (1993); (b) N. Nakamura, T. Hanasaki, H. Onoi, T. Oida. *Chem. Express*, **8**, 467 (1993); (c) T. Hanasaki, M. Ueda, N. Nakamura. *Mol. Cryst. liq. Cryst.*, **237**, 329 (1993); (d) N. Nakamura, H. Onoi, T. Hanasaki. *Mol. Cryst. liq. Cryst.*, **257**, 43 (1994); (e) N. Nakamura, T. Oida, M. Shonago, T. Hanasaki. *Mol. Cryst. liq. Cryst.*, **265**, 1 (1995).

[10] M. Moriyama, S. Song, N. Tamaoki. *J. Mater. Chem*, **11**, 1003 (2001).

[11] D. Apreutesei, G. Lisa, H. Akutsu, N. Hurduc, S. Nakatsuji, D. Scutaru. *Appl. Organometal. Chem*, **19**, 1022 (2005).

[12] K.-Q. Zhao, P. Hu, H.-B. Xu. *Molecules*, **6**, M246 (2001).

[13] P.J. Collings, M. Hird. In *Introduction to Liquid Crystal Chemistry and Physics*, G.W. Gray, J.W. Goodby, A. Fukuda (Eds), Taylor and Francis, London. 148 (1997).

[14] B.I. Ostovskii. *Liq. Cryst*, **14**, 131 (1993).

[15] D. Apreutesei, D. Scutaru, G.H. Mehl. paper presented at the 16th Conference on Liquid Crystals, Stare Jablonki, Poland, September (2005).

[16] D. Apreutesei, G. Lisa, N. Hurduc, D. Scutaru. paper presented at Troisieme Colloque Franco-Roumain de Chimie Appliquee, Slanic Moldova, Romania (2004).

[17] P. Hu, K.-Q. Zhao, H.B. Xu. *Molecules*, **6**, M250 (2001).